Kinetic Modeling of Radical Thiol–Ene Chemistry for Macromolecular Design: Importance of Side Reactions and Diffusional Limitations

ARTICLE *in* MACROMOLECULES · MARCH 2013

Impact Factor: 5.8 · DOI: 10.1021/ma302619k

7 AUTHORS, INCLUDING:

Pieter Espeel
Ghent University
28 PUBLICATIONS **792** CITATIONS
SEE PROFILE

Bryan Marin
Ghent University
401 PUBLICATIONS **4,825** CITATIONS
SEE PROFILE

Filip Du Prez
Ghent University
209 PUBLICATIONS **4,862** CITATIONS
SEE PROFILE

Macromolecules

Article

pubs.acs.org/Macromolecules

Kinetic Modeling of Radical Thiol–Ene Chemistry for Macromolecular Design: Importance of Side Reactions and Diffusional Limitations

Pieter Derboven,[†] Dagmar R. D'hooge,[†] Milan M. Stamenovic,[‡] Pieter Espeel,[‡] Guy B. Marin,[†] Filip E. Du Prez,*[,‡] and Marie-Françoise Reyniers*[,†]

[†]Laboratory for Chemical Technology, Ghent University, Ghent B-9000, Belgium

[‡]Polymer Chemistry Research Group, Ghent University, Ghent B-9000, Belgium

Supporting Information

ABSTRACT: The radical thiol–ene coupling of thiol-functionalized polystyrene (PS-SH) with dodecyl vinyl ether (DVE) and the polystyrene-*b*-poly(vinyl acetate) (PS-*b*-PVAc) polymer–polymer conjugation using 2,2-dimethoxy-2-phenylacetophenone (DMPA) as photoinitiator are modeled to assess the importance of diffusional limitations and side reactions. Intrinsic chemical rate coefficients are determined based on a kinetic study of the coupling of benzyl thiol (BT) and DVE. The addition and transfer reactions are chemically controlled, whereas diffusional limitations on termination slightly increase the coupling efficiency. Termination by recombination of carbon-centered radicals and addition of DMPA derived radicals to DVE are shown to be mainly responsible for the reduced coupling efficiency in case polymeric species are involved. The obtained results confirm the idea to disregard radical thiol–ene chemistry as a true member of the family of "click" chemistry techniques for polymer–polymer conjugation and show that the initial conditions have a significant impact on the coupling efficiency.

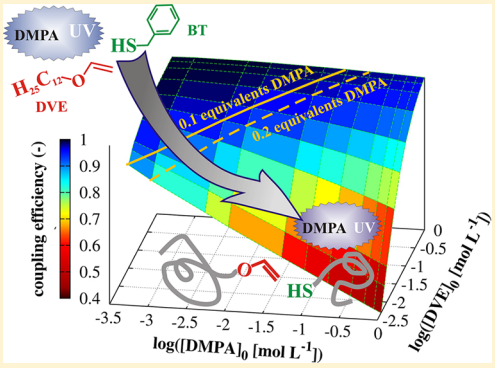

INTRODUCTION

Recent research[1−3] has shown that the "click" chemistry concept allows the efficient and straightforward synthesis of advanced polymer architectures. Using this concept, complex macromolecular architectures can be formed by coupling macromolecules, ideally with high yield, excellent modularity, and orthogonality under a variety of mild conditions. In addition, for a true "click" reaction inoffensive byproducts are easily removable via nonchromatographic methods.[4]

Over the past decade, the Huisgen Cu(I)-catalyzed 1,3-dipolar cycloaddition of alkynes and azides[5] has evolved as the norm for "click"-termed reactions, in particular when tailored design features are required, as is the case for the synthesis of functionalized polymers and polymer–polymer conjugates.[6−8] Despite its very high reaction rate, the Cu(I)-mediated "click" reaction suffers from toxicity issues related to the employed catalyst. Therefore, significant efforts have been devoted to the exploitation of metal-[6] and additive-free[9] "click" reactions, extending the realm of the "click" philosophy to, among others, (hetero-)Diels–Alder reactions,[8,9] radical and nucleophilic thiol–ene[10−13] chemistry, and ultrarapid synthetic approaches such as norbornene–tetrazine chemistry.[14]

Within the large repertoire of these new "click" chemistry approaches, the radical addition of thiyl radicals ($R_1S^•$) to nonactivated double bonds ($CH_2{=}CHR_2$), i.e. thiol–ene reactions,[15] offers in principle the combination of high efficiency, good robustness, and oxygen[16] and water tolerance, starting from commercially available compounds. In particular, UV-initiated thiol–ene "click" chemistry enables an unique spatial and temporal control with applications in the fields of materials science and synthetic chemistry, including surface and polymer modification, biofunctionalization, and uniform network formation.[11,13]

The principle of the UV-initiated thiol–ene process is shown in Scheme 1. Initially, carbon-centered radicals are generated by cleavage of a photoinitiator (I_1I_2), typically 2,2-dimethoxy-2-phenylacetophenone (DMPA),[17] and subsequent transfer to the thiol (R_1SH) leads to the formation of thiyl radicals ($R_1S^•$), which in turn can add to an ene molecule ($CH_2{=}CHR_2$). The desired thio–ether coupling product is formed, once the resulting carbon-centered radical abstracts a hydrogen from another thiol molecule. In this last step, a new thiyl radical is formed, allowing further reaction if the ene-containing species is still present. In case of DMPA, applied wavelengths typically are close to the visible light (λ = 365 nm), implying the possibility to generate thiyl radicals using sunlight as radiation source.[18,19] Interestingly, thiol–ene chemistry can even be conducted in the absence of a photoinitiator, as specific thiols lead to self-initiation at a well-chosen wavelength (e.g., alkyl 3-mercaptopropionate at λ = 254 nm).[20,21]

Ideally, the final thio–ether coupling product concentration should be equal to the initial ene or thiol concentration

Received: December 21, 2012
Revised: February 4, 2013
Published: February 21, 2013

Scheme 1. Principle of UV-Initiated Thiol−Ene "Click" Chemistry[a]

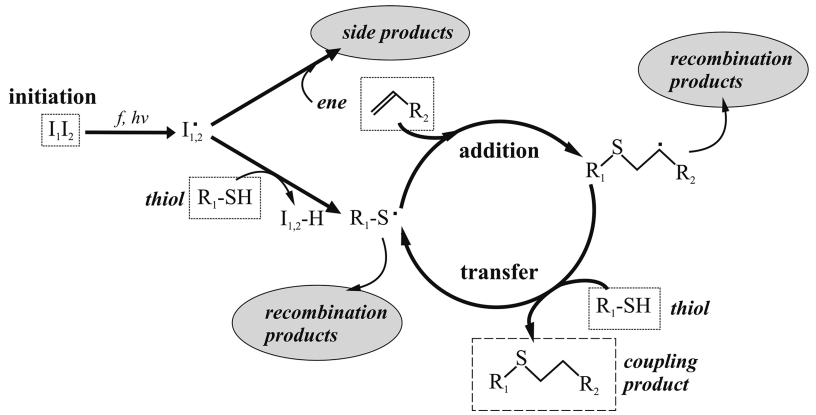

[a]R_1 and R_2: low or high molar mass compound; side reactions are indicated in gray.

depending on the ene or thiol being the limiting reagent, and a coupling efficiency of 100% should therefore be obtained. However as indicated in Scheme 1, several side reactions can interfere, leading to a reduced coupling efficiency. For example, consumption of the ene compound might occur via homopolymerization if a (homo)polymerizable ene, such as an acrylate,[22] is used or via addition of photoinitiator derived radicals to the ene. Also, termination reactions can interrupt the thiol−ene coupling process, among which thiyl−thiyl radical coupling, head-to-head coupling of the carbon-centered radicals, and cross-termination between carbon-centered and thiyl radicals are the most prominent termination reactions.[23]

The mechanism of the radical thiol−ene chemistry presented in Scheme 1 suggests that the overall kinetics might be first order in both the initial thiol and ene concentration. However, differential scanning calorimetry (DSC) and Fourier transform infrared (FTIR) monitoring of radical thiol−ene reactions[23,24] indicate that different vinyl compounds exhibit different overall reaction orders and that the overall rates mainly depend on the ratio of the addition to the transfer rate coefficient $k_{add,chem}/k_{tr,chem}$. For the thiol−allyl ether system, the overall reaction order was even observed to be independent of the initial ene concentration and could be very well described by a $k_{add,chem}$ to $k_{tr,chem}$ ratio of 10.[23,24] Contrary to these experimental findings, a recent quantum-chemical study reported by Northrop and Coffey[25] suggests a ratio of $k_{add,chem}$ to $k_{tr,chem}$ lower than 1 for the thiol−allyl ether system and that for thiol−propene, thiol−vinyl ether, thiol−vinylsilazane, and thiol−allyl ether the overall reaction rate might be slowed down considerably due to the occurrence of the β C−S scission reaction, i.e., the reverse of the addition reaction. However, Reddy et al.[24,26] were able to model conversion−time profiles for a range of thiol−ene systems without the need to consider the occurrence of the reverse β C−S scission.

Recently, Koo et al.[19] employed thiol−ene chemistry in combination with reversible addition−fragmentation chain transfer (RAFT) polymerization[27−29] to assess its potential as a tool for polymer functionalization as well as star polymer and block copolymer synthesis. However, when targeting conjugation of thiol-functionalized polystyrene (PS-SH) and allyl ether-functionalized poly(vinyl acetate) (PVAc), nuclear magnetic resonance (NMR) spectroscopy and elemental analysis revealed only a limited success of the radical-initiated thiol−ene reaction (coupling efficiency: ∼25%), particularly in case equimolar starting prepolymer concentrations were used, as required by the adapted macromolecular "click" definition.[30] In addition, size exclusion chromatography (SEC) analysis suggested the undesired formation of termination products. Also, the star polymer assembly of a poly(butyl acrylate) macromonomer with a trimethylolpropane tris(2-mercaptoacetate) trifunctional thiol core was only successful to a small extent, as indicated by mass spectrometry and SEC analysis. In a first attempt to explain these observations, the authors proposed that unwanted termination by recombination reactions and addition of photoinitiator derived radicals to the ene as well as a diffusion-controlled addition reaction could contribute to the reduction of the coupling efficiency. Because of the lack of an extensive set of experimental data, these hypotheses could unfortunately not be attested.

Kinetic simulations by Preuss and Barner-Kowollik[31] revealed that diffusional effects might indeed play a role in polymer−polymer conjugation. In case the coupling reactivity for low molar mass species is similar as for termination (10^9 L mol^{-1} s^{-1}), the obtained molar mass distribution (MMD) displays a marked conversion dependence with the effect being most pronounced for initially broad MMDs. Based on literature reports, the DMPA photoinitiated radical thiol−ene polymer−polymer conjugation can thus be expected to be influenced both by side reactions and diffusional limitations on the reaction rates. However, it remains unclear to which extent each of these phenomena influence the coupling efficiency.

In this work, a combined experimental and modeling study is presented, allowing to assess the main factors controlling the coupling efficiency in radical thiol−ene reactions photoinitiated by DMPA. As model compounds, benzyl thiol (BT), dodecyl vinyl ether (DVE), thiol-functionalized polystyrene (PS-SH) and allyl ether-functionalized poly(vinyl acetate) are considered, the macromolecular compounds being the same as in the earlier study of Koo et al.[19] It is shown that both for coupling of small species and coupling reactions involving polymeric species the coupling efficiency crucially depends on the chosen reaction conditions. Lower initial concentrations of the ene and thiol compound and higher initial photoinitiator concentrations decrease the ratio of the addition/transfer rate to the photoinitiator decomposition rate, thus favoring the formation of side products. Furthermore, the lower coupling efficiencies for polymer−polymer conjugation cannot be attributed to diffusional limitations on addition and transfer reactions, since their intrinsic reactivity is too low as compared to termination reactions.

dx.doi.org/10.1021/ma302619k | Macromolecules 2013, 46, 1732−1742

EXPERIMENTAL SECTION

Materials. Dodecyl vinyl ether (DVE; 98% pure) and dibenzyl disulfide (BDS; 98% pure) were purchased from Sigma-Aldrich. Benzyl thiol (BT; 99% pure) and the solvent 1,4-dioxane (>99.5% pure, inhibitor free) were purchased from Acros Organics. As a radical source, 2,2-dimethoxy-2-phenylacetophenone (DMPA; Acros Organics) was used. All chemicals were used as received.

Methods. *Analysis.* A VLX365 radiometer (bandwidth: 355−375 nm) was used to measure the intensity profile of the UV lamps (setup with nine Philips PL-S 9 W UV-A lamps, bandwidth: 340−400 nm and maximum at 365 nm), while the temperature profiles of the sample mixtures during reaction were measured with a digital VWR thermometer (EU 620-0919). For the coupling of DVE and BT, online Fourier transform infrared (FTIR; carbon−carbon double bond stretch absorbance peak at 1620 cm^{-1}; Mettler Toledo ReactIR 4000), gas chromatography (GC; Hewlett-Packard (Agilent) 5890; flame ionization detector), and 300 MHz ^1H nuclear magnetic resonance (^1H NMR; Bruker Avance 300) analyses were performed. A Hewlett-Packard GCD-Plus GC/MS (G1800B; MS: mass spectrometry) was used for qualitative characterization of the samples.

Coupling Reaction between BT and DVE (Small−Small). An overview of the experiments performed is given in Table 1 (entries 1−3). For a typical experiment (e.g., entry 1 in Table 1; infrared (IR) detection) first, DMPA (1.0×10^{-5} mol, 2.55 mg) is dissolved in 4.5 mL of 1,4-dioxane in a 25 mL two-necked, glass flask. Then, DVE (1.4×10^{-3} mol, 0.37 mL) is added, and after attaching the flask to an IR-probe, the obtained mixture is purged with argon for 30 min and stirred at 800 rpm. After 30 min, BT (1.4×10^{-3} mol, 0.17 mL) is added. In case GC is used as an analysis method, an additional 15 μL of the internal standard *n*-dodecane (DD) is added. The sample is purged for another 20 min and afterwards irradiated for 10 min with 365 nm UV-light.

Table 1. Overview of Reaction Conditions Used for the Kinetic Study of the Coupling of Benzyl Thiol (BT) and Dodecyl Vinyl Ether (DVE) in 1,4-Dioxane, Photoinitiated by 2,2-Dimethoxy-2-phenylacetophenone (DMPA) (T = 21 °C; Irradiation Time = 10 min)

entry	components	$[thiol]_0/[ene]_0$	$[ene]_0$ (mol L^{-1})	$[DMPA]_0$[a] (mol L^{-1})	v_{sol}[b] (%)
1	BT/DVE/DMPA	1	0.3	0.002	89
2	BT/DVE/DMPA	0.5	0.4	0.002	87
3	BT/DVE/DMPA	2	0.2	0.002	90
4	BDS/DMPA[c]			0.004	∼100

[a]In entries 2−4, 0.01 equiv of DMPA with respect to limiting reacting agent (i.e., thiol, ene, or benzyl disulfide (BDS)) is used, whereas in entry 1 this value is 0.0067. [b]v_{sol}: volume percentage of solvent in the sample. [c]Concentration of BDS/DMPA: 0.004 mol L^{-1}.

To study disulfide dissociation/formation in the absence of ene or thiol (entry 4 in Table 1), a similar approach as for entries 1−3 in Table 1 is followed as explained in section S.3 of the Supporting Information.

In the present kinetic study, reliable analysis under maximum light intensity during the entire reaction was not possible due to practical reasons and the change of the intensity of the UV lamps had therefore to be taken into account in the kinetic model (see section S1 of the Supporting Information). Furthermore, no significant temperature increase of the mixture during the coupling reaction was measured, which allows to assume isothermal conditions for the kinetic modeling study and determination of the intrinsic chemical rate coefficients.

Kinetic Model. Similar to the work of Cramer et al.[23,24] and Back et al.,[15] kinetic modeling is used as a tool to study the coupling reaction between BT and DVE. However, in this work a more extended reaction scheme, including the reverse β C−S scission as proposed by Northrop and Coffey,[25] is considered. The model thus allows to assess the importance of the reverse reaction for the addition step. Furthermore, it enables to study the effect of side reactions with photoinitiator-derived radicals and to determine the influence of diffusional limitations on the coupling efficiency ($f_{coupling}$), which is defined as the molar ratio of the concentration of the thio−ether coupling product ($c_{thio-ether}$) to the initial concentration of the limiting reagent ($c_{thiol,0}$ or $c_{ene,0}$):

$$f_{coupling} = \frac{c_{thio-ether}}{c_{ene,0}} \quad \text{or} \quad f_{coupling} = \frac{c_{thio-ether}}{c_{thiol,0}} \tag{1}$$

In addition, for macromolecular species the coupling reaction should be ideally performed using equimolar initial concentrations of the ene and thiol groups.[30] It should be kept in mind that the definition given in eq 1 only holds when the limiting reagent reaches full conversion during the time span of the considered reaction. An alternative definition is presented by eq 2, in which the obtained coupling product concentration is related to the amount of limiting reagent that has been consumed. However, throughout this article eq 1 will be used, since this quantity is directly accessible by ^1H NMR analysis for the studied system.

$$f'_{coupling} = \frac{c_{thio-ether}}{c_{ene,0} - c_{ene}} \quad \text{or} \quad f'_{coupling} = \frac{c_{thio-ether}}{c_{thiol,0} - c_{thiol}} \tag{2}$$

A detailed description of the kinetic model and its assumptions are given in section S4 of the Supporting Information. The corresponding intrinsic chemical rate coefficients are taken from literature (see section S4 in Supporting Information) or determined based on experimental data as discussed below.

RESULTS AND DISCUSSION

In this section, it is first explained how approximate values for the intrinsic kinetic parameters are obtained for the BT/DVE small−small model system. Next, the influence of the initial concentrations on the coupling efficiency and the side product spectrum for this small−small model system is illustrated. Finally, it is demonstrated that coupling reactions involving polymeric species are not influenced by diffusional limitations on addition nor transfer. The reduced coupling efficiency for polymer−small and polymer−polymer conjugations is shown to be mainly due to an increased importance of termination reactions with carbon-centered radicals and of addition reactions involving photoinitiator-derived radicals. The latter is a direct consequence of the lower applied initial ene and thiol concentrations due to the limited solubility of the polymers.

Coupling of BT and DVE (Small−Small). As mentioned above, the coupling of BT and DVE has been monitored using online FTIR and GC. Figure 1 (entry 1 in Table 1) shows that online FTIR (squares) and GC (triangles) measurements lead to the same DVE conversion profile. For the online FTIR measurements, the carbon−carbon double bond stretch absorbance peak at 1620 cm^{-1} is tracked, while for GC analysis

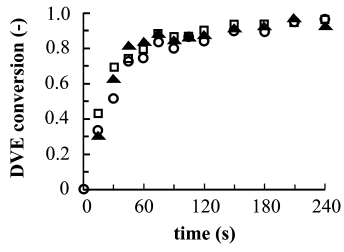

Figure 1. Conversion profiles of dodecyl vinyl ether (DVE) determined by online Fourier transform infrared (FTIR; squares), gas chromatography (GC; triangles), and 300 MHz proton nuclear magnetic resonance (^1H NMR; circles); entry 1 in Table 1.

dx.doi.org/10.1021/ma302619k | Macromolecules 2013, 46, 1732−1742

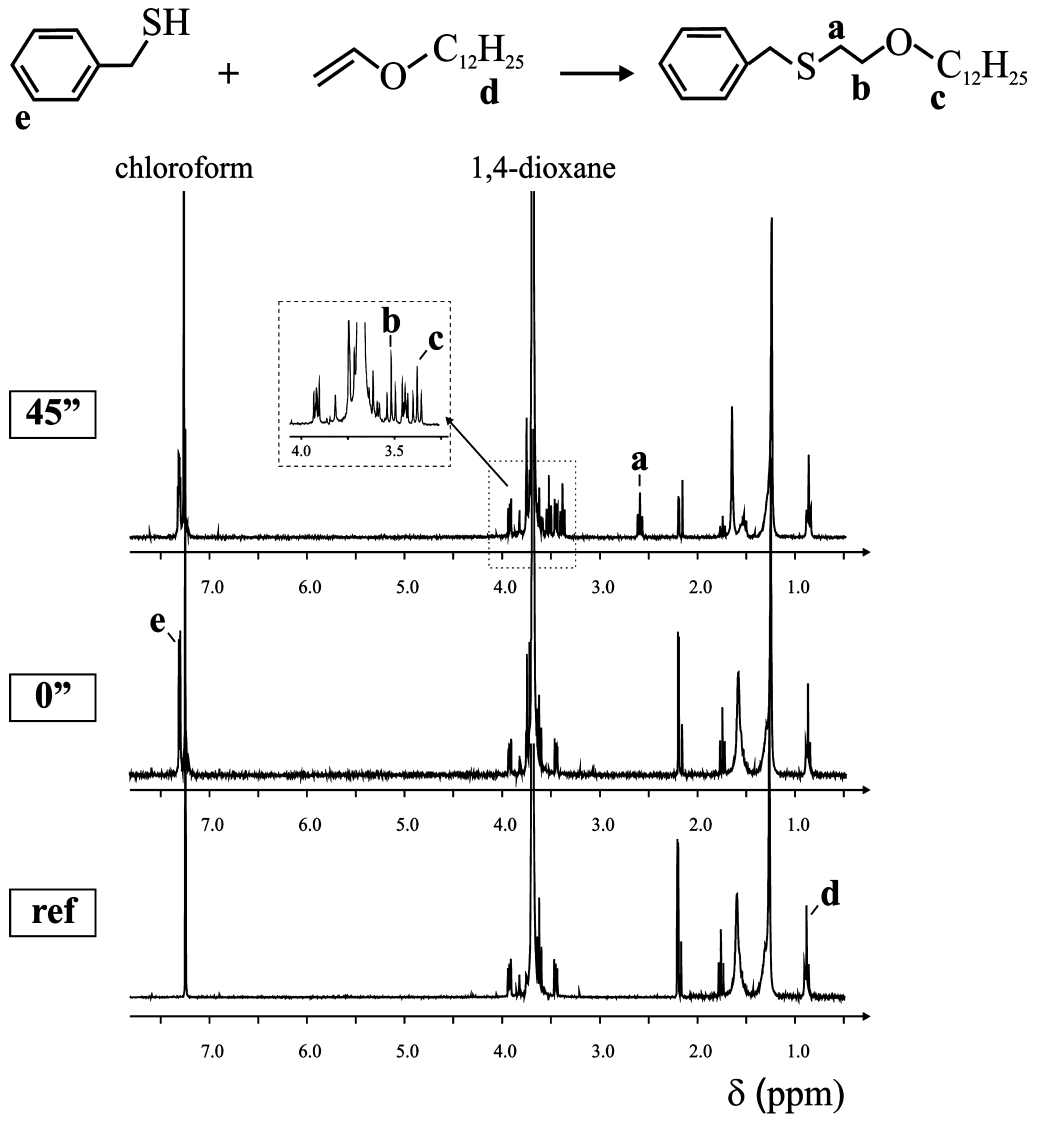

Figure 2. Overlay of the proton nuclear magnetic resonance (^{1}H NMR) 300 MHz reference spectrum: dodecyl vinyl ether (DVE)/2,2-dimethoxy-2-phenylacetophenone (DMPA)/1,4-dioxane (ref), the spectrum just before the reaction (0″), and the spectrum after 45 s of reaction (45″); conditions: entry 1, Table 1.

the ratio of the DVE peak to the internal standard peak (DD) is compared to the initial ratio.

The 300 MHz ^{1}H NMR overlay of the reference spectrum (before BT was added: DVE/DMPA/1,4-dioxane; ref), the spectrum just before reaction (0″), and the spectrum after 45 s of reaction (45″) are shown in Figure 2. The peaks corresponding to 1,4-dioxane, BT, and DVE are labeled. The coupling efficiency is calculated by relating the area of peak a, which is the resonance signal of the two hydrogens next to the thio−ether bond (see Figure 2), to the area of peak d, which corresponds to the methyl hydrogens at the tail of the dodecyl group in the DVE molecule. A coupling efficiency of 100% is obtained at sufficiently high reaction time (around 4 min), so that its corresponding time profile can be used as extra measurement for the conversion−time profile of DVE or BT. As can be seen in Figure 1, this profile (circles) is in good agreement with the FTIR (squares) and GC (triangles) results.

Figures 3a−c show the experimentally measured and simulated DVE conversion profiles (full lines) for an initial molar ratio of BT to DVE of 2, 1, and 0.5 (entries 1−3 in Table 1). It can be observed that a good description of the experimental DVE conversion data is obtained for all three conditions. Moreover, an excellent description of the photoinitiator conversion under typical coupling conditions (entry 1 in Table 1) results, as shown in Figure 4.

For the intrinsic rate coefficient for the addition of BT to DVE ($k_{add,chem}$) and the intrinsic rate coefficient for the subsequent transfer reaction yielding the thio−ether coupling product ($k_{tr,chem}$), values of 1.2×10^6 and 1.1×10^6 L mol^{-1} s^{-1} are respectively obtained, which are similar to those reported by Reddy et al.[22,26] It should be stressed that the measured DVE conversion data allow a reliable assessment of these intrinsic chemical rate coefficients, since diffusional limitations can be neglected for the coupling reaction between the low molar mass compounds BT and DVE and isothermicity holds (see Experimental Section). Although Northrop and Coffey[25] highlighted the importance of the β C−S scission reaction for vinyl ether coupling reactions, simulations revealed that a proper description of the experimental conversion data recorded in this work is not possible using their reported rate

dx.doi.org/10.1021/ma302619k | Macromolecules 2013, 46, 1732−1742

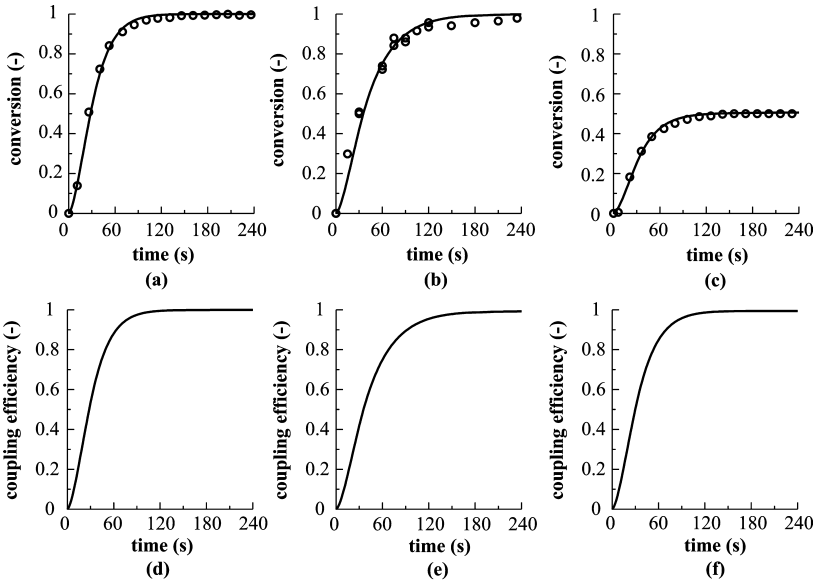

Figure 3. Dodecyl vinyl ether (DVE) conversion (full line) and the coupling efficiency (eq 1) as a function of time for (a/d) entry 3 in Table 1, $[BT]_0/[DVE]_0 = 2$; (b/e) entry 1 in Table 1, $[BT]_0/[DVE]_0 = 1$; (c/f) entry 2 in Table 1, $[BT]_0/[DVE]_0 = 0.5$; points: experimental data; line: simulated using the kinetic parameters in Table S1; BT = benzylthiol.

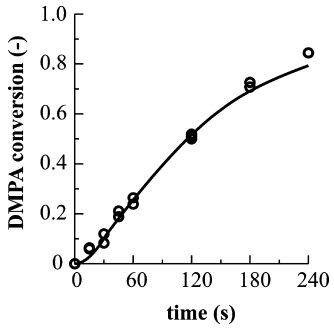

Figure 4. Conversion of the photoinitiator as a function of time; conditions: entry 1 in Table 1; points: experimental data; line: simulated using the parameters in Table S1.

coefficients. However, since these authors focused on methyl vinyl ether/methyl mercaptan instead of DVE/BT,[25] the importance of the β C−S scission reaction is re-evaluated from the equilibrium coefficient for the addition/ β C−S scission calculated using Benson's group additivity method.[32] A very high value for the equilibrium coefficient of 10^{11} L mol^{-1} results, indicating that the addition of the thiyl radical to the double bond of DVE can be considered as irreversible and, hence, that the β C−S scission can indeed be safely neglected for the BT/DVE system (see section S5 of the Supporting Information).

The values of the other intrinsic kinetic parameters are discussed in section S4 of the Supporting Information. Except for termination by recombination, literature data are used.[22,33,34] The intrinsic chemical rate coefficients for termination by recombination ($k_{tc,chem}$) are determined from an independent experiment (entry 4 in Table 1), in which a known amount of dibenzyl disulfide (BDS) and DMPA are dissolved in 1,4-dioxane in the absence of DVE and BT, followed by irradiation at the same wavelength used in an actual thiol−ene coupling experiment (UV, λ = 365 nm). The concentration of BDS during the irradiation period is monitored using GC, and the resulting concentration−time profile is shown in Figure 5 (points). As explained in section S3 of the Supporting Information, additionally, GC/MS measurements are performed to identify the different products at varying irradiation times.

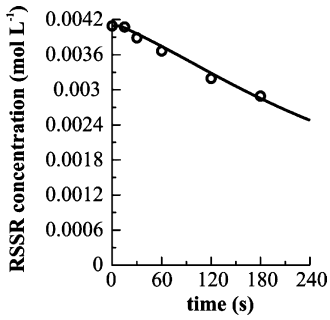

Figure 5. Concentration of dibenzyl disulfide as a function of time (entry 4 in Table 1); points: experimental data; line: simulated using kinetic parameters in Table S1.

The experiment is designed based on the observations of Sayamol et al.,[35] who reported the UV-induced dissociation of disulfides. Since the results of Reddy et al.[22,26] imply that, in a first approximation, the intrinsic chemical recombination rate coefficients in the DVE/BT system can be assumed equal, the experimental data in Figure 5 allow the determination of the intrinsic rate coefficient $k_{tc,chem}$ taking into account that mainly recombination reactions between the thiyl and the photoinitiator radicals occur (see section S3 of the Supporting Information). Using a value of 4×10^9 L mol^{-1} s^{-1} for $k_{tc,chem}$, a good agreement between experiment and simulation is obtained, as shown in Figure 5. Furthermore, this value is in agreement with the early work of Fischer et al.[36] and the more recent evaluation of the intrinsic termination rate coefficient of small radicals by Smith et al.[37] The photodissociation parameters considered in the kinetic model for this specific experiment are discussed in sections S1 and S3 of the Supporting Information.

dx.doi.org/10.1021/ma302619k | Macromolecules 2013, 46, 1732−1742

The simulated coupling efficiencies (eq 1) for entries 1−3 in Table 1 are shown in Figure 3d−f. On the basis of these results, it can be concluded that the coupling reaction of BT and DVE shows "click" characteristics, since values of ca. 100% are obtained under equimolar conditions (entry 1 in Table 1), in agreement with the 300 MHz ^{1}H NMR data (Figures 1 and 2). However, as illustrated in Figure 6, simulations reveal that even

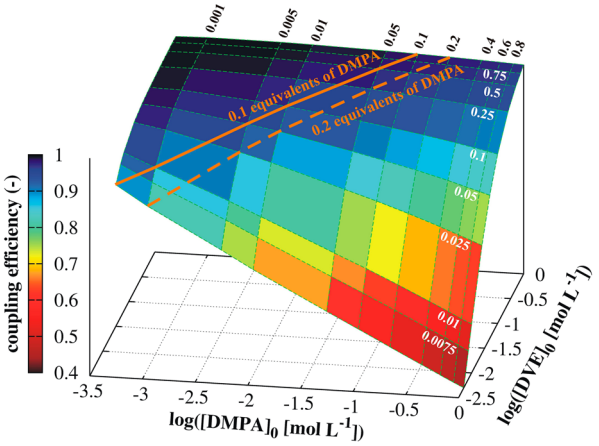

Figure 6. Final coupling efficiency as a function of the logarithm of the initial photoinitiator (2,2-dimethoxy-2-phenylacetophenone, DMPA) and ene (dodecyl vinyl ether, DVE) concentration; the absolute initial concentrations of the ene and the photoinitiator (mol L^{-1}) have been added as well on the surface for clarity; coupling efficiency: eq 1; simulated using the parameters in Table S1; T = 21 °C, reaction performed in 1,4-dioxane; final = full ene conversion.

for the small−small BT/DVE/DMPA system, the coupling efficiency crucially depends on the applied initial concentrations. This figure shows that at full ene conversion both an increase of the initial photoinitiator concentration and/or a decrease of the initial ene concentration significantly reduce the coupling efficiency for an equimolar radical thiol−ene reaction. Clearly, the highest coupling efficiencies are obtained for initial ene/thiol concentrations greater than 0.1 mol L^{-1} and photoinitiator concentrations lower than 0.05 mol L^{-1}. A further decrease of the initial ene and/or thiol concentration or an increase of the initial photoinitiator concentration induce an increased formation of side products (see further) and hence reduce the coupling efficiency, as also shown in Figure 7 in which a two-dimensional projection of Figure 6 for the initial

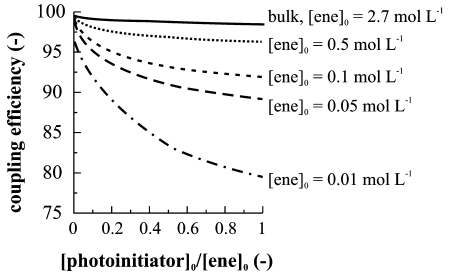

Figure 7. Final coupling efficiency as a function of the initial initiator to ene molar ratio for various initial ene concentrations for the dodecyl vinyl ether (DVE)/benzyl thiol (BT)/2,2-dimethoxy-2-phenylacetophenone (DMPA) model system in 1,4-dioxane; in all simulations equimolar amounts of ene and thiol are used; bulk: isothermal conditions assumed, T = 21 °C; final = full ene conversion.

concentration range typically applied in synthetic chemistry is presented. Additionally in Figure 6, the coupling efficiencies corresponding to typically applied initial photoinitiator to ene molar ratios, i.e. 0.1 and 0.2, are indicated. It follows that such conditions allow a high coupling efficiency (>0.8).

It is important to realize that a proper understanding of the effect of the initial concentrations on the coupling efficiency is crucial with regard to radical thiol−ene reactions involving polymeric species. In such reactions, the limited solubility of the polymer species directly determines the initial end-group concentrations for the ene/thiol species that can be used in the coupling reaction. Typically, the initial concentration of the polymeric species is some 10 times lower than the initial concentrations used for small−small coupling reactions. Hence, from Figure 6, an increased importance of the occurrence of side reactions is expected when going from typical small−small conditions (≥0.1 mol L^{-1}) to conditions in which polymeric species are involved (0.01−0.05 mol L^{-1}).

The observed trend in Figure 6 can be understood by taking into account that the photodecomposition of DMPA is unimolecular, while the addition and transfer rates are bimolecular. Hence, a typical 10-fold decrease of the initial concentrations of ene, thiol, and photoinitiator when going from small−small radical thiol−ene reactions to coupling reactions involving polymeric species will have a more pronounced effect on the addition and transfer rates. This difference in decrease between the radical generation rate by photoinitiation and the rate at which the radicals react to yield the desired coupling product indeed favors the formation of side products. The latter is illustrated in Figure 8 for two initial conditions which are typical for small−small (Figure 8a,b) and polymer−polymer (Figure 8c,d) thiol−ene coupling reactions. Although the initial DMPA to ene molar ratio remains unchanged, i.e., 0.2, lowering of the initial ene/thiol concentration from 0.3 mol L^{-1} (Figure 8a,b) to 0.03 mol L^{-1} (Figure 8c,d) implies that the relative contribution of side products increases (Figure 8b,d). In particular, it can be seen that the formation of recombination products and products derived from addition of photoinitiator radicals to the ene increases with increasing overall dilution.

Moreover, this decrease in the initial concentrations results in an important increase of the photoinitiator conversion from 20 to 60% (Figure 8e; full and dotted line, right axis) at full consumption of the ene, leading to a lower selectivity of the thiyl radical toward addition on the ene double bond (Figure 8f; full and dotted line) and a concomitant reduction of the coupling efficiency (Figure 8e; full and dotted line, left axis).

It can thus be concluded that a small−small radical thiol−ene coupling reaction only shows "click" characteristics when sufficiently low initial photoinitiator and sufficiently high initial ene/thiol concentrations are used.

Polymeric Thiol−Ene Reactions: Coupling of PS-SH and DVE (Polymer Functionalization). When BT is replaced by its macromolecular analogue, i.e., thiol-functionalized polystyrene (PS-SH), Koo et al.[19] reported a coupling efficiency of ∼90% for the coupling with DVE photoinitiated by DMPA ($[DMPA]_0/[PS\text{-}SH]_0$ = 0.2). Such value was measured both in case a 5-fold excess and an equimolar amount of DVE were used. These authors suggested that diffusional limitations and side reactions, such as termination and addition of photoinitiator-derived radicals, might be responsible for the reduced coupling efficiency. However, these hypotheses could not be validated from the experimental data. To evaluate the

dx.doi.org/10.1021/ma302619k | Macromolecules 2013, 46, 1732−1742

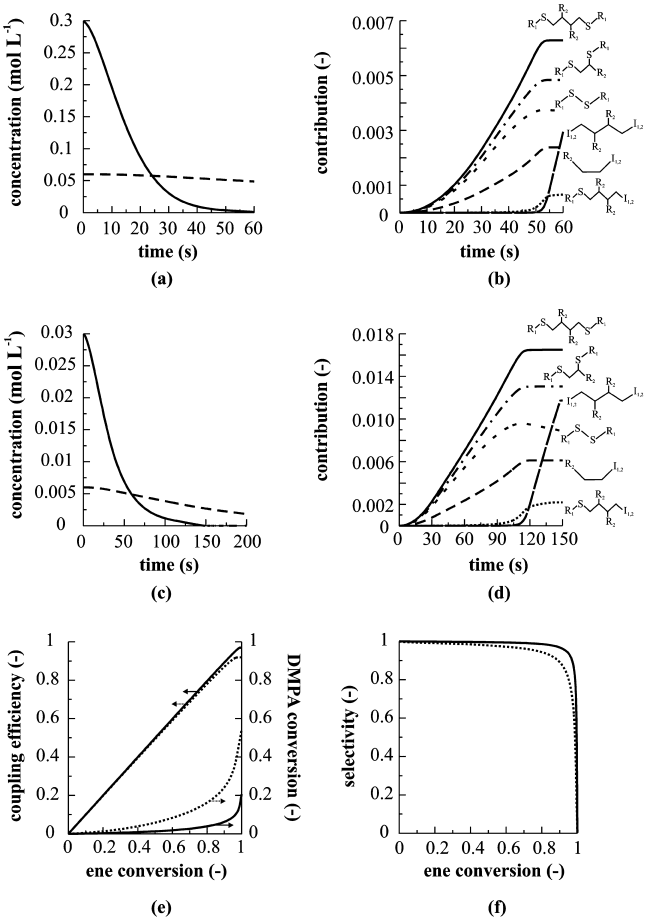

Figure 8. Concentration of ene (full line; dodecyl vinyl ether, DVE), photoinitiator (dashed line; 2,2-dimethoxy-2-phenylacetophenone, DMPA), and contribution of main side products as a function of time; molar ratio of photoinitiator to ene of 0.2; (a/b) $[ene]_0$ = $[thiol]_0$ = 0.3 mol L^{-1} and (c/d) $[ene]_0$ = $[thiol]_0$ = 0.03 mol L^{-1}; (b/d) contribution = concentration of the corresponding side product normalized with respect to the initial DVE concentration; (e) coupling efficiency and DMPA conversion as function of ene conversion (full line: conditions (a/b), dotted line: conditions (c/d)); (f) selectivity of the thiyl radical toward addition on the ene double bond (full line: conditions (a/b), dotted line: conditions (c/d)); reaction performed in 1,4-dioxane.

effect of diffusional control on the coupling efficiency, the kinetic model was extended to account for diffusional limitations on termination, addition, and transfer reactions. For termination reactions, a power law approach was used:[37,38]

$$k_{tc,app}^{ii} = k_{tc,app}^{11} i^{-\alpha} \quad (3)$$

in which $k_{tc,app}^{ii}$ is the apparent rate coefficient for termination by recombination of macromolecules of chain length i in dilute solution and α is a fitting parameter available in the literature. α is taken equal to 0.5 as reported for PS radicals in the short chain length regime.[38] It should however be stressed that for high chain lengths (i > 50) its value decreases to 0.15, and hence, its beneficial effect on the coupling efficiency will be less pronounced. In this work, for $k_{tc,app}^{11}$ the value obtained for the coupling reaction between BT and DVE (small−small) is used. For further details the reader is referred to section S6 of the Supporting Information. It has to be emphasized that diffusional limitations on termination lead to increased values of the coupling efficiency.

For the other reactions involving macromolecular species (addition and transfer), no power law model is available to assess the importance of diffusional limitations, and the encounter pair model[39−42] is used instead:

$$\frac{1}{k_{app,1}} = \frac{1}{k_{chem,1}} + \frac{1}{k_{diff,1}} \quad (4)$$

In eq 4, $k_{diff,l}$ and $k_{chem,l}$ are the diffusional and intrinsic chemical rate coefficient of the considered reaction 1. For the calculation of $k_{diff,l}$ the reader is referred to section S6 of the Supporting Information. On the other hand, $k_{chem,l}$ can be assessed based on the corresponding small−small system, i.e., BT/DVE, taking into account a typical chain length dependency when going from nonmacromolecular to macromolecular species.

Several literature reports[43−46] indicate a decrease of the intrinsic addition rate coefficient by 1 order of magnitude when going from a small species to a polymer chain consisting of more than ca. 10 monomer units, which is mainly attributed to differences in the pre-exponential Arrhenius factor. A similar chain length dependency is expected for transfer reactions, as the pre-exponential Arrhenius factors of both addition and transfer reactions are determined by similar physical parameters.[45,47] Therefore, in this kinetic model a 10-fold lower reactivity of macroradicals toward addition and transfer reactions has been assumed, taking into account that the average chain length of the polymer molecules is 40.[19] Hence, for $k_{add,chem}^{macro}$ and $k_{tr,chem}^{macro}$, intrinsic values of 1.2 × 10^5 and 1.1 × 10^5 L mol^{-1} s^{-1} are considered, respectively.

However, both intrinsic chemical rate coefficients are too low to be influenced by diffusional limitations. They are 4 orders of magnitude lower (~10^5 L mol^{-1} s^{-1}) than for termination (~10^9 L mol^{-1} s^{-1}) refuting, for the studied system, the hypothesis of Koo et al.,[19] which states that diffusional limitations on the addition reaction could explain the reduced coupling efficiency when macromolecular species are involved. Only in case addition and transfer reactions have an intrinsic chemical rate coefficient of ca. 10^8−10^9 L mol^{-1} s^{-1}, the lower mobility of longer macromolecules can lead to a diffusion controlled coupling.[31]

In Table 2, the simulated final coupling efficiency, as obtained by a kinetic model considering the chain length dependency of $k_{add,chem}^{macro}$ and $k_{tr,chem}^{macro}$ (CLD) on the one hand and neglecting this dependency (CLI) on the other are compared with the experimental data of Koo et al.[19] for the coupling of PS-SH with DVE. It follows that the former assumption results in a slight underestimation of the experimental coupling

Table 2. Final Coupling Efficiency (Eq 1) for Thiol-Functionalized Polystyrene (PS-SH)/Dodecyl Vinyl Ether (DVE) (Polymer Functionalization)[a]

	experimental		simulation	
entry	$[DVE]_0/[PS\text{-}SH]_0$	$f_{coupling}$	$f_{coupling}$ (CLD): k_{chem}^{macro}	$f_{coupling}$ (CLI): k_{chem}
1	1	~0.90	0.82	0.97
2	5	~0.90	0.87	0.98

[a] M_n/PDI of PS-SH: 4000 g mol^{-1}/1.20; intrinsic kinetic parameters: Table S1 in Supporting Information; diffusion parameters: see section S6 of the Supporting Information; reaction time: 1 h; $[PS\text{-}SH]_0$ = 0.05 mol L^{-1}; $[DMPA]_0$ = 0.01 mol L^{-1} (0.2 equiv with respect to PS-SH); DMPA = 2,2-dimethoxy-2-phenylacetophenone; final = full ene conversion.

dx.doi.org/10.1021/ma302619k | Macromolecules 2013, 46, 1732−1742

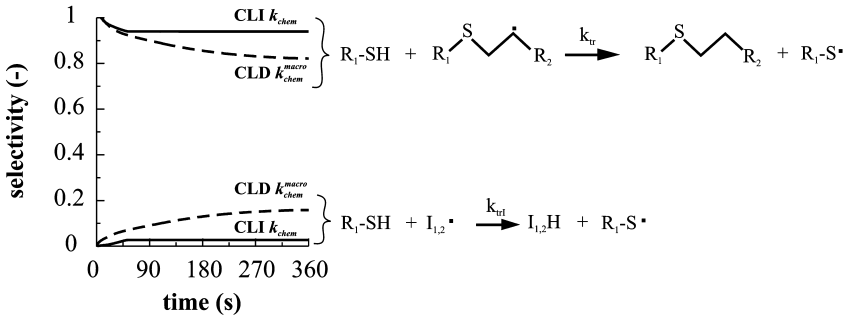

Figure 9. Selectivity of the thiol R_1-SH (Scheme 1) toward transfer reactions with photoinitiator-derived radicals and carbon-centered radicals leading to the coupling product, for both chain length dependent (CLD) and independent (CLI) addition and transfer rate coefficients; R_1: polystyrene chain, R_2: $OC_{12}H_{25}$; results shown until full conversion of the ene; conditions: entry 1 in Table 2.

efficiency, whereas the latter clearly leads to an overestimation, favoring the consideration of a chain length dependent addition and transfer reaction in agreement with literature reports.[43−46]

In other words, Table 2 demonstrates that a reduction of the intrinsic rate coefficients for addition and transfer affects the coupling efficiency significantly. Bearing in mind the above discussion, this can be easily understood since a lowering of the rate coefficients for addition and transfer directly reduces the addition and transfer rates while the initiation rate remains unaffected.

This leads to a favoring of side reactions, as illustrated in Figure 9, which shows a higher selectivity of the thiol for transfer reaction with a photoinitiator-derived radical than for an intermediate carbon-centered radical leading to the desired coupling product, in case chain length dependent addition and transfer rate coefficients are assumed. Note that the selectivity is defined as the fraction of the consumed thiol molecules that have reacted via the corresponding reaction pathway.

Furthermore, as already anticipated by Koo et al.,[19] Figure 10 demonstrates that coupling of intermediate carbon-centered

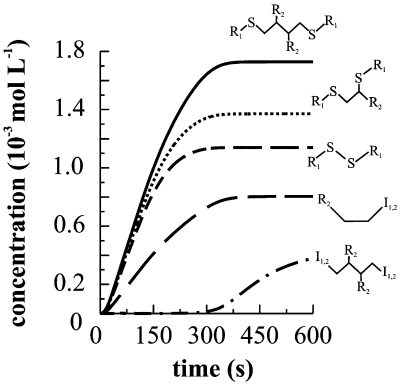

Figure 10. Concentration of the main side products as a function of time; R_1: polystyrene chain, R_2: $OC_{12}H_{25}$; results shown until full conversion of the ene; conditions: entry 1 in Table 2 (CLD) with final simulated coupling efficiency of 0.82.

radicals is the main termination pathway, whereas addition of initiator radicals to the ene compound has a significant contribution to the loss of coupling efficiency as well.

Hence, it can be concluded that the reduced coupling efficiency for the PS-SH/DVE system, compared to the BT/DVE system, is mainly caused by the occurrence of side reactions with photoinitiator fragments and termination by recombination reactions, whereas diffusional limitations on addition and transfer reactions can be neglected. Moreover, these side reactions are a direct consequence of the lower applied initial concentrations and the reduction of the addition and transfer rate coefficients due to their chain length dependency, both leading to a significant decrease of the addition and transfer rates, whereas the rate at which radicals are generated by photodecomposition of the initiator is affected less. Additionally, it can be anticipated that similar factors explain the failure of the star formation synthesis starting from a poly(butyl acrylate) macromonomer and a trifunctional thiol, as observed by Koo et al.[19]

Polymeric Thiol−Ene Reactions: Polymer−Polymer Conjugation (PS-*b*-PVAc). Koo et al.[19] reported a reduced coupling efficiency of ca. 25% for the conjugation of equimolar amounts (0.03 mol L^{-1}) of an allyl ether-functionalized poly(vinyl acetate) (PVAc, M_n = 1800 g mol^{-1}, PDI = 1.5) segment and a PS-SH (M_n = 4000 g mol^{-1}, PDI = 1.2) segment using an initial molar ratio of photoinitiator to ene equal to 0.2. However, as it is impossible to quantify experimentally the different polymer−polymer and polymer-initiator radical adducts, simulations are necessary to explain the strong reduction of the coupling efficiency. From the previous simulation results involving PS-SH, it can be expected that the low polymer−polymer coupling yield can be attributed to a high importance of termination by recombination reactions and side reactions with photoinitiator radicals, confirming the hypothesis of Koo et al.[19]

In the kinetic model the chain length dependency of the addition and transfer rate coefficients is taken into account, and the ratio between both is set equal to 10 based on the results of Cramer et al.[23,24] A 10 times lower reactivity toward transfer allows to reproduce the experimental trends, which is however not the case when the rate coefficients reported by Northrop and Coffey[25] for methyl allyl ether/methyl mercaptan are used. In particular, the rate coefficients calculated by Northrop and Coffey[25] result in an overall reaction rate being dependent both on the ene and the thiol concentration, while for an allyl ether system the overall reaction rate is experimentally observed to be independent of the initial ene concentration.[23,24] Therefore, to evaluate the importance of the β C−S scission reaction, the equilibrium coefficient for the addition/β C−S scission reaction has again been calculated using Benson's group additivity method.[32] An equilibrium coefficient of 10^2 L mol^{-1} (see section S5 in Supporting Information) results, implying a higher importance of the β C−S scission reaction than for the vinyl ether system. Hence, combined with the known value for the addition rate coefficient, the rate coefficient for the β C−S scission is obtained. Simulation results confirm that this

dx.doi.org/10.1021/ma302619k | Macromolecules 2013, 46, 1732−1742

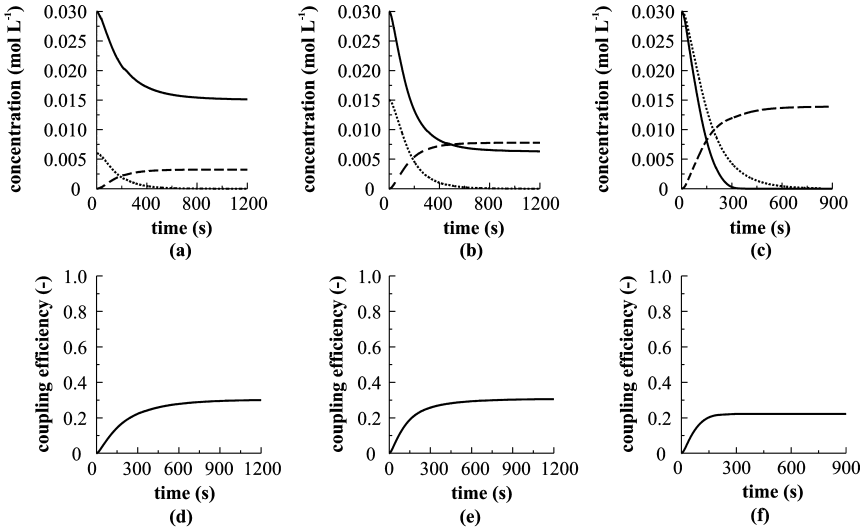

Figure 11. Concentration of the ene (full line; coinciding with the thiol profile), the photoinitiator (dotted line), and the total concentration of the main side products (dashed line) as a function of time for equimolar coupling of thiol-functionalized polystyrene (PS-SH) and allyl ether-functionalized poly(vinyl acetate) (PVAc); $[PS\text{-}SH]_0 = [PVAc]_0 = 0.03$ mol L^{-1} (a) $[photoinitiator]_0 = 0.006$ mol L^{-1} (0.2 equiv), (b) $[photoinitiator]_0 = 0.015$ mol L^{-1} (0.5 equiv) and (c) $[photoinitiator]_0 = 0.03$ mol L^{-1} (1 equiv); (d–f) corresponding coupling efficiency as a function of time.

approach did not affect the zero-order dependency of the overall reaction rate on the initial ene concentration, while the values of the other rate coefficients are taken the same as determined for the vinyl ether system.[22,26]

It has to be stressed that also for this polymer–polymer system diffusional limitations are only important on termination reactions, which lead to increased values of the coupling efficiency. Since the transfer and addition reactions are even more chemically controlled, the reduced mobility when shifting from the polymer–small to the polymer–polymer system cannot explain the limited coupling efficiency. On the contrary, the low initial applied concentrations of the thiol and ene polymeric species due to their limited solubility, and the reduced reactivity toward transfer compared to the vinyl ether system, are the actual reasons for the limited coupling efficiency. Both factors result in a decrease of the addition and transfer rates and, as highlighted above, lead to an increased selectivity for side reactions. This is further illustrated in Figure 11d, which shows the simulated coupling efficiency as a function of time for the conditions mentioned above. A final coupling efficiency of 0.3 is obtained, which is close to the experimental one of 0.25. Although the same initial conditions have been applied as for the simulations in Figure 8e (dotted line) for the small–small system (BT/DVE/DMPA), the significant reduction of the coupling efficiency from 0.9 (Figure 8e, dotted line) to 0.3 (Figure 11d) is solely attributed to the above indicated decrease in reactivity toward addition and transfer.

Furthermore, Figure 11a clearly indicates that the low coupling efficiency cannot be completely attributed to side reactions, since no full conversion of the ene and thiol (full line) is reached during the time span of complete decomposition of the photoinitiator (dotted line) for the considered condition. It should be stressed that both the experimentally determined coupling efficiency via ^{1}H NMR and the simulated efficiencies in Figure 11d–f correspond to the definition in eq 1, implying that an incomplete conversion of the ene or thiol would also lead to a reduction of the coupling efficiency.

To reach full conversion of the thiol and ene compound, and aspiring in that way a higher coupling efficiency, it could be expected that a higher initial photoinitiator concentration might be beneficial. However, Figure 11d–f shows that increasing the initial photoinitiator concentration does not lead to the desired increase of the coupling efficiency in spite of the increased conversion of the thiol and ene compound (Figure 11a–c; full line). In line with the observations for the small molecule system (BT/DVE/DMPA; Figure 6), simulations revealed that a higher initial photoinitiator concentration favors side product formation and thus reduces the coupling efficiency even more. This can also be derived from Figure 11a–c, in which the total concentration of the main side products is also plotted as a function of reaction time (dashed line).

In addition, as shown in section S7 of Supporting Information, the carbon–carbon coupling of intermediate carbon-centered radicals is the main side reaction, in agreement with the simulations results on the coupling of PS-SH/BT and DVE. It is also shown in section S6 that the addition of photoinitiator-derived radicals to the ene and its subsequent transfer and recombination product(s) have a significant contribution.

Finally, in Figure 12 the effect of stepwise addition of small amounts of photoinitiator (DMPA) on the coupling efficiency is evaluated. It can be seen that somewhat higher coupling efficiencies can be obtained (~50%), since this approach allows to reach full ene conversion while keeping the photoinitiator concentration low. However, simulations in which the initial photoinitiator concentration, the amount of photoinitiator added, and the frequency of the addition were varied revealed a maximal coupling efficiency of only 60%. This implies that even with stepwise addition of the photoinitiator high coupling efficiencies can never be achieved.

Hence, it can be concluded that photoinitiated radical thiol–ene chemistry is not an efficient way to synthesize block copolymers when making use of an allyl ether end-group functionality. A more reactive end group, such as norbornene, can increase the coupling efficiency, as was recently addressed

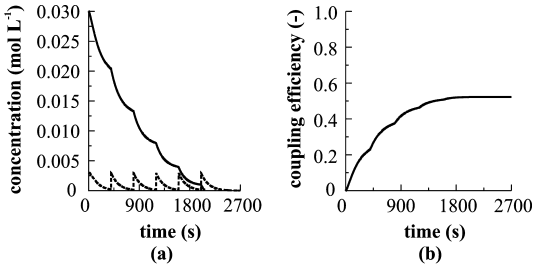

Figure 12. Equimolar coupling of thiol-functionalized polystyrene (PS-SH) and allyl ether-functionalized poly(vinyl acetate) PVAc; $[PS\text{-}SH]_0 = [PVAc]_0 = 0.03$ mol L^{-1}. (a) Concentration of the initiator (dashed line) and ene compound (full line) versus time. (b) Coupling efficiency versus time; $[initiator]_0 = 0.003$ mol L^{-1}; stepwise addition of initiator every 400 s.

by Stamenovic et al.,[48] although side reactions will still be inevitable.

CONCLUSIONS

Kinetic modeling is used to understand the reduced coupling efficiency for the functionalization reaction of PS-SH with DVE and the PS-*b*-PVAc polymer–polymer conjugation, photoinitiated by DMPA. The simulations show that the reduced coupling efficiencies cannot be attributed to a diffusion-controlled addition or transfer reaction but are caused by an increased importance of in particular termination by recombination reactions and addition of the DMPA derived radicals to the ene compound, as previously proposed by Koo et al.[19]

This study also revealed that even for small–small systems the coupling efficiency crucially depends on the choice of the reaction conditions. Too high initial concentrations of photoinitiator and too low initial ene/thiol concentrations enhance the occurrence of side reactions. The limited coupling efficiency for polymer–polymer thiol–ene conjugation can hence be traced back to the limited solubility of polymeric species and the resulting low end-group concentrations.

In principle, a higher coupling efficiency can be achieved by stepwise addition of DMPA, as full conversion of the thiol and ene compound can be reached while maintaining a low DMPA concentration. However, the obtained coupling product yields are still far away from the desired 100%, confirming that radical thiol–ene chemistry has to be excluded as a true member of the family of "click" chemistry techniques for polymer–polymer conjugation.

ASSOCIATED CONTENT

Supporting Information

Determination of the molar absorptivity of DMPA in 1,4-dioxane at 365 nm; recorded intensity versus time profile of the UV-lamps used; experimental procedure, GC(/MS) analysis results, and determination of kinetic parameters for the UV-induced dissociation of benzyl disulfide in the presence of DMPA in 1,4-dioxane; model assumptions and a complete list of all the reactions considered in the kinetic model together with the values of the corresponding rate coefficients; calculation of the equilibrium coefficients for the addition/β C–S-scission via Benson's group additivity method, including a list of the literature-based group additive values necessary for the calculation; evaluation of diffusional limitations for both the addition/transfer and the termination reactions in case macromolecular species are involved; plot of the main side products as a function of time for polymer–polymer conjugation. This material is available free of charge via the Internet at http://pubs.acs.org.

AUTHOR INFORMATION

Corresponding Author

*E-mail: MarieFrancoise.Reyniers@UGent.be (M.-F.R.); Filip.Duprez@UGent.be (F.E.D.).

Notes

The authors declare no competing financial interest.

ACKNOWLEDGMENTS

The Institute for the Promotion of Innovation through Science and Technology in Flanders (IWT Vlaanderen), the Fund for Scientific Research Flanders (FWO), the Long Term Structural Methusalem Funding by the Flemish Government, and the Interuniversity Attraction Poles Programme initiated by the Belgian State, the Prime Minister's office (IAP/IUAP/PAI P7/05: "Functional Supramolecular Systems") and the European Science Foundation–Precision Polymer Materials (P2M) program are acknowledged for financial support.

NOMENCLATURE

Cu(I) copper atom, oxidation state +I
I_1I_2 photoinitiator which dissociates upon UV-radiation yielding the radical fragments I_1 and I_2
RSH general thiol molecule
RS general thiyl radical
$R_{1,2}$ low or high molar mass compound
$[thiol]_0$ initial thiol concentration (mol L^{-1})
$[ene]_0$ initial concentration of ene compound (mol L^{-1})
$[I_1I_2]$ concentration of photoinitiator (mol L^{-1})
f photoinitiator efficiency
h the Planck constant (J s)
N_A the Avogadro constant (mol^{-1})
$f_{coupling}$ coupling efficiency (−)
I irradiation intensity (mW cm^{-2} s^{-1})
c speed of light (m s^{-1})

Greek Symbols

λ wavelength (nm)
ν frequency (s^{-1})
ε molar absorptivity (L mol^{-1} s^{-1})
α fitting parameter (−)

Abbreviations

UV ultraviolet light
DVE dodecyl vinyl ether
DMPA 2,2-dimethoxy-2-phenylacetophenone
BT benzyl thiol
PS polystyrene
PS-SH thiol-functionalized polystyrene
PVAc poly(vinyl acetate)
DD *n*-dodecane
CRP controlled radical polymerization
RAFT reversible addition–fragmentation chain transfer
NMR nuclear magnetic resonance
SEC size exclusion chromatography
FTIR Fourier transform infrared
GC gas chromatography
MS mass spectroscopy
EPR electron paramagnetic resonance
MMD molar mass distribution
THF tetrahydrofuran

BDS benzyl disulfide
rpm rotations per minute
vol % volume percentage (−)
LSODA Livermore Solver for Ordinary Differential Equations
PDI polydispersity index
CLD chain length dependent
CLI chain length independent

Subscripts

sol solvent
I regarding initiator (derived) species
chem intrinsic chemical (contribution)
add addition
tr transfer
tc termination by recombination

Superscripts

i, *j* chain length
macro macromolecular

REFERENCES

(1) Binder, W. H.; Sachsenhofer, R. *Macromol. Rapid Commun.* **2007**, *28*, 15−54.
(2) Binder, W. H.; Sachsenhofer, R. *Macromol. Rapid Commun.* **2008**, *29*, 952−981.
(3) Moses, J. E.; Moorhouse, A. D. *Chem. Soc. Rev.* **2007**, *36*, 1249−1262.
(4) Kolb, H. C.; Finn, M. G.; Sharpless, K. B. *Angew. Chem., Int. Ed.* **2001**, *40*, 2004−2021.
(5) Rostovtsev, V. V.; Green, L. G.; Fokin, V. V.; Sharpless, K. B. *Angew. Chem., Int. Ed.* **2002**, *41*, 2596−2599.
(6) Becer, C. R.; Hoogenboom, R.; Schubert, U. S. *Angew. Chem., Int. Ed.* **2009**, *48*, 4900−4908.
(7) Hansell, C. F. E., P.; Stamenovic, M. M.; Barker, I. A.; Dove, A. P.; Du Prez, F. E.; O'Reilly, R. K. *J. Am. Chem. Soc.* **2011**, *133*, 13828−13831.
(8) Tasdelen, M. A. *Polym. Chem.* **2011**, *2*, 2133−2145.
(9) Hizal, G.; Tunca, U.; Sanyal, A. *J. Polym. Sci., Part A: Polym. Chem.* **2011**, *49*, 4103−4120.
(10) Hoyle, C. E.; Bowman, C. N. *Angew. Chem., Int. Ed.* **2010**, *49*, 1540−1573.
(11) Hoyle, C. E.; Lee, T. Y.; Roper, T. *J. Polym. Sci., Part A: Polym. Chem.* **2004**, *42*, 5301−5338.
(12) Kade, M. J.; Burke, D. J.; Hawker, C. J. *J. Polym. Sci., Part A: Polym. Chem.* **2010**, *48*, 743−750.
(13) Hoyle, C. E.; Lowe, A. B.; Bowman, C. N. *Chem. Soc. Rev.* **2010**, *39*, 1355−1387.
(14) Inglis, A. J.; Barner-Kowollik, C. *Macromol. Rapid Commun.* **2010**, *31*, 1247−1266.
(15) Back, R. M., C.; Sivertz, C. *Can. J. Chem.* **1954**, *32*, 1078−1091.
(16) Kharasch, M. N., W.; Mantell, G. *J. Org. Chem.* **1951**, *16*, 524−532.
(17) Uygun, M.; Tasdelen, M. A.; Yagci, Y. *Macromol. Chem. Phys.* **2010**, *211*, 103−110.
(18) ten Brummelhuis, N.; Diehl, C.; Schlaad, H. *Macromolecules* **2008**, *41*, 9946−9947.
(19) Koo, S. P. S.; Stamenovic, M. M.; Prasath, R. A.; Inglis, A. J.; Du Prez, F. E.; Barner-Kowollik, C.; Van Camp, W.; Junkers, T. *J. Polym. Sci., Part A: Polym. Chem.* **2010**, *48*, 1699−1713.
(20) Cramer, N. B.; Reddy, S. K.; Cole, M.; Hoyle, C.; Bowman, C. N. *J. Polym. Sci., Part A: Polym. Chem.* **2004**, *42*, 5817−5826.
(21) Cramer, N. B.; Scott, J. P.; Bowman, C. N. *Macromolecules* **2002**, *35*, 5361−5365.
(22) Reddy, S. K.; Cramer, N. B.; Bowman, C. N. *Macromolecules* **2006**, *39*, 3681−3687.
(23) Cramer, N. B.; Davies, T.; O'Brien, A. K.; Bowman, C. N. *Macromolecules* **2003**, *36*, 4631−4636.
(24) Cramer, N. B.; Reddy, S. K.; O'Brien, A. K.; Bowman, C. N. *Macromolecules* **2003**, *36*, 7964−7969.
(25) Northrop, B. H.; Coffey, R. N. *J. Am. Chem. Soc.* **2012**, *134*, 13804−13817.
(26) Reddy, S. K.; Cramer, N. B.; Bowman, C. N. *Macromolecules* **2006**, *39*, 3673−3680.
(27) Moad, G.; Rizzardo, E.; Thang, S. H. *Polymer* **2008**, *49*, 1079−1131.
(28) Chiefari, J.; Chong, Y. K.; Ercole, F.; Krstina, J.; Jeffery, J.; Le, T. P. T.; Mayadunne, R. T. A.; Meijs, G. F.; Moad, C. L.; Moad, G.; Rizzardo, E.; Thang, S. H. *Macromolecules* **1998**, *31*, 5559−5562.
(29) Roth, P. J.; Boyer, C.; Lowe, A. B.; Davis, T. P. *Macromol. Rapid Commun.* **2011**, *32*, 1123−1143.
(30) Barner-Kowollik, C.; Du Prez, F. E.; Espeel, P.; Hawker, C. J.; Junkers, T.; Schlaad, H.; Van Camp, W. *Angew. Chem., Int. Ed.* **2011**, *50*, 60−62.
(31) Preuss, C. M.; Barner-Kowollik, C. *Macromol. Theory Simul.* **2011**, *20*, 700−708.
(32) Poling, B. E.; Prausnitz, J. M.; O'Connell, J. P. *The Properties of Gases and Liquids*; McGraw-Hill: New York, 2001.
(33) Colley, C. S.; Grills, D. C.; Besley, N. A.; Jockusch, S.; Matousek, P.; Parker, A. W.; Towrie, M.; Turro, N. J.; Gill, P. M. W.; George, M. W. *J. Am. Chem. Soc.* **2002**, *124*, 14952−14958.
(34) Hristova, D.; Gatlik, I.; Rist, G.; Dietliker, K.; Wolf, J. P.; Birbaum, J. L.; Savitsky, A.; Mobius, K.; Gescheidt, G. *Macromolecules* **2005**, *38*, 7714−7720.
(35) Sayamol, K.; Knight, A. R. *Can. J. Chem.* **1968**, *46*, 999−1003.
(36) Fischer, H.; Paul, H. *Acc. Chem. Res.* **1987**, *20*, 200−206.
(37) Smith, G. B.; Russell, G. T.; Heuts, J. P. A. *Macromol. Theory Simul.* **2003**, *12*, 299−314.
(38) Barner-Kowollik, C.; Russell, G. T. *Prog. Polym. Sci.* **2009**, *34*, 1211−1259.
(39) Gilbert, R. G. *Pure Appl. Chem.* **1992**, *64*, 1563−1567.
(40) D'Hooge, D. R.; Reyniers, M.-F.; Marin, G. B. *Macromol. React. Eng.* **2009**, *3*, 185−209.
(41) D'Hooge, D. R.; Reyniers, M.-F.; Stadler, F. J.; Dervaux, B.; Bailly, C.; Du Prez, F. E.; Marin, G. B. *Macromolecules* **2010**, *43*, 8766−8781.
(42) De Roo, T.; Wieme, J.; Heynderickx, G. J.; Marin, G. B. *Polymer* **2005**, *46*, 8340−8354.
(43) Fischer, H.; Radom, L. *Angew. Chem., Int. Ed.* **2001**, *40*, 1340−1371.
(44) Heuts, J. P. A.; Russell, G. T. *Eur. Polym. J.* **2006**, *42*, 3−20.
(45) Heuts, J. P. A.; Russell, G. T.; Smith, G. B. *Aust. J. Chem.* **2007**, *60*, 754−764.
(46) Gridnev, A. A.; Ittel, S. D. *Macromolecules* **1996**, *29*, 5864−5874.
(47) Heuts, J. P. A. In *Handbook of Radical Polymerization*; Matyjaszewski, K., Davis, T. P, Eds.; Wiley and Sons: New York, 2002; pp 1−76.
(48) Stamenovic, M. M.; Espeel, P.; Van Camp, W.; Du Prez, F. E. *Macromolecules* **2011**, *44*, 5619−5630.